J|A|C|S
ARTICLES
Published on Web 12/20/2007

OFF−OFF−ON Switching of Fluorescence and Electron Transfer Depending on Stepwise Complex Formation of a Host Ligand with Guest Metal Ions

Junpei Yuasa and Shunichi Fukuzumi*

Department of Material and Life Science, Division of Advanced Science and Biotechnology, Graduate School of Engineering, Osaka University, SORST, Japan Science and Technology Agency (JST), Suita, Osaka 565-0871, Japan

Received July 2, 2007; E-mail: fukuzumi@chem.eng.osaka-u.ac.jp

Abstract: Stepwise complex formation is observed between 2,3,5,6-tetrakis(2-pyridyl)pyrazine (TPPZ) and a series of metal ions (M^{n+} = Sc^{3+}, Y^{3+}, Ho^{3+}, Eu^{3+}, Lu^{3+}, Nd^{3+}, Zn^{2+}, Mg^{2+}, Ca^{2+}, Ba^{2+}, Sr^{2+}, Li^{+}), where TPPZ forms a 2:1 complex [$(TPPZ)_2-M^{n+}$] and a 1:1 complex [$TPPZ-M^{n+}$] with M^{n+} at low and high concentrations of metal ions, respectively. The fluorescence intensity of TPPZ begins to increase at high concentrations of metal ions, when the 2:1 $(TPPZ)_2-M^{n+}$ complex is converted to the fluorescent 1:1 $TPPZ-M^{n+}$ complex. This is regarded as an "OFF−OFF−ON" fluorescence sensor for metal ions depending on the stepwise complex formation between TPPZ and metal ions. The fluorescence quantum yields of the $TPPZ-M^{n+}$ complex vary depending on the metal valence state, in which the fluorescence quantum yields of the divalent metal complexes ($TPPZ-M^{2+}$) are much larger than those of the trivalent metal complexes ($TPPZ-M^{3+}$). On the other hand, the binding constants of $(TPPZ)_2-M^{n+}$ (K_1) and $TPPZ-M^{n+}$ (K_2) vary depending on the Lewis acidity of metal ions (i.e., both K_1 and K_2 values increase with increasing Lewis acidity of metal ions). Sc^{3+}, which acts as the strongest Lewis acid, forms the $(TPPZ)_2-Sc^{3+}$ and $TPPZ-Sc^{3+}$ complexes stoichiometrically with TPPZ. In such a case, "OFF−OFF−ON" switching of electron transfer from cobalt(II) tetraphenylporphyrin (CoTPP) to O_2 is observed in the presence of Sc^{3+} and TPPZ depending on the ratio of Sc^{3+} to TPPZ. Electron transfer from CoTPP to O_2 occurs at Sc^{3+} concentrations above the 1:2 ratio ($[Sc^{3+}]/[TPPZ]_0 > 0.5$), when the $(TPPZ)_2-Sc^{3+}$ complex is converted to the $TPPZ-Sc^{3+}$ complex and $TPPZ-(Sc^{3+})_2$, which act as promoters of electron transfer (ON) by the strong binding of $O_2^{\bullet-}$ with Sc^{3+}. In sharp contrast, no electron transfer occurs without metal ion (OFF) or in the presence at Sc^{3+} concentrations below the 1:2 ratio (OFF), when the $(TPPZ)_2-Sc^{3+}$ complex has no binding site available for $O_2^{\bullet-}$.

Introduction

Fluorescence sensors for metal ions are one of the common analytical tools for obtaining quantitative information about the amount of those metal ions,[1−5] where a probe molecule recognizes a metal ion to emit specific fluorescence upon binding of the metal ion.[1−5] Simple 1:1 stoichiometric host (probe molecules or ligands)−guest (metal ions) recognition has been a general pattern of complex formation in fluorescence sensor, affording "OFF−ON" switchability (Scheme 1a). The fluorescence intensity due to the 1:1 complex formation with the metal ion (M^{n+}) increases linearly with increasing metal ion concentration from 0 M ($[M^{n+}] > 0$ M). In such a case, however, those fluorescence sensors bind with metal ions within only a limited concentration range of metal ions.

In contrast to the simple 1:1 complex formation, a stepwise complex formation (2:1 and 1:1) in host (probe molecules or ligands)−guest (metal ions) recognition would afford nonlinear "OFF−OFF−ON" switchability in fluorescence sensors provided that only the 1:1 complex is fluorescent (Scheme 1b). In such a case, a probe molecule begins to fluoresce at certain concentrations of metal ions, when the 2:1 complex starts to be

(1) (a) de Silva, A. P.; Gunaratne, H. Q. N.; Gunnlaugsson, T.; Huxley, A. J. M.; McCoy, C. P.; Rademacher, J. T.; Rice, T. E. *Chem. Rev.* **1997**, *97*, 1515. (b) Tsien, R. Y. In *Fluorescent Chemosensors for Ion and Molecule Recognition*; Czarnik, A. W., Ed.; ACS Symposium Series 538; American Chemical Society: Washington, DC, 1993.

(2) (a) Jiang, P.; Guo, Z. *Coord. Chem. Rev.* **2004**, *248*, 205. (b) Rurack, K.; Resch-Genger, U. *Chem. Soc. Rev.* **2002**, *31*, 116.

(3) (a) Aoki, S.; Kawatani, H.; Goto, T.; Kimura, E.; Shiro, M. *J. Am. Chem. Soc.* **2001**, *123*, 1123. (b) Corneillie, T. M.; Whetstone, P. A.; Fisher, A. J.; Meares, C. F. *J. Am. Chem. Soc.* **2003**, *125*, 3436. (c) Saha, A. K.; Kross, K.; Kloszewski, E. D.; Upson, D. A.; Toner, J. L.; Snow, R. A.; Black, C. D. V.; Desai, V. C. *J. Am. Chem. Soc.* **1993**, *115*, 11032. (d) Balzani, V.; Lehn, J.-M.; van de Loosdrechi, J.; Mecati, A.; Sabbatini, N.; Ziessel, R. *Angew. Chem., Int. Ed. Engl.* **1991**, *30*, 190. (e) Saudan, C.; Balzani, V.; Gorka, M.; Lee, S.-K.; Maestri, M.; Vicinelli, V.; Vögtle, F. *J. Am. Chem. Soc.* **2003**, *125*, 4424. (f) de Silva, A. P.; Fox, D. B.; Huxley, A. J. M.; McClenaghan, N. D.; Roiron, J. *Coord. Chem. Rev.* **1999**, *185*−*186*, 297. (g) Okamoto, K.; Fukuzumi, S. *J. Am. Chem. Soc.* **2004**, *126*, 13922.

(4) For PET sensors, see: (a) de Silva, A. P.; Gunaratne, H. Q. N.; McCoy, C. P. *Nature* **1993**, *364*, 42. (b) Ghosh, P.; Bharadwaj, P. K.; Roy, J.; Ghosh, S. *J. Am. Chem. Soc.* **1997**, *119*, 11903. (c) Ramachandram, B.; Saroja, G.; Sankaran, N. B.; Samanta, A. *J. Phys. Chem. B* **2000**, *104*, 11824. (d) Burdette, S. C.; Walkup, G. K.; Springler, B.; Tsien, R. Y.; Lippard, S. J. *J. Am. Chem. Soc.* **2001**, *123*, 7831. (e) James, T. D.; Linnane, P.; Shinkai, S. *Chem. Commun.* **1996**, 281.

(5) Either a red or blue shift in emission in response to concentration of metal ion has been reported. See: Wilson, J. N.; Bunz, U. H. F. *J. Am. Chem. Soc.* **2005**, *127*, 4124.

 10.1021/ja0748480 CCC: $40.75

Scheme 1

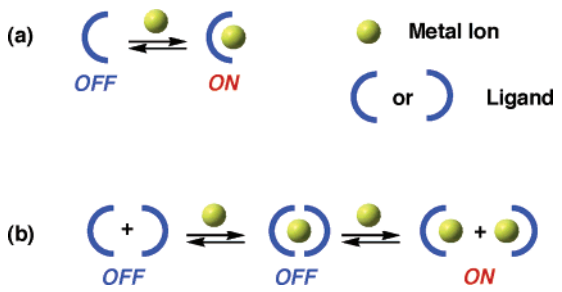

converted to the 1:1 complex. This is potentially quite useful for routine analysis of metal ions in a broad concentration range,[6] because development of detection tools for metal ions in a broad concentration range (such as Zn^{2+} in a cellular system, where its concentration varies over a wide range from 10^{-10} to 10^{-4} M in some vesicles) has been highly desired.[7−9]

The complex formation of host ligands with guest metal ions also affects metal ion-promoted electron-transfer reactions from electron donors to acceptors. It has been reported that the electron-transfer processes are accelerated by binding of metal ion complexes (Lewis acids) with the product radical anions of electron acceptors (Lewis bases).[10−19] The Lewis acidity of metal ion complexes can be regulated by host ligands acting as Lewis bases.[18,19] In the case of 1:1 complex formation (Scheme 2a),

Scheme 2

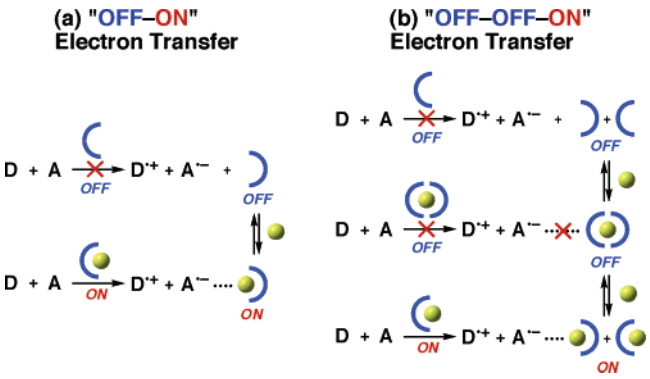

the rates of electron transfer increase linearly with increasing concentrations of metal ions from 0 M ($[M^{n+}] > 0$ M) as the case of fluorescence sensor (Scheme 1a). In contrast, a stepwise complex formation (2:1 and 1:1) between ligands and metal ions would afford nonlinear "OFF−OFF−ON" switchability of electron transfer provided that only the 1:1 metal ion complex can activate electron transfer by coordination of the products of electron transfer to a vacant site of metal ion complexes (Scheme 2b). It has been suggested that new frontiers of electron transfer are exploited in such nonlinear dynamics.[20−22] Nonlinear kinetics has thus far been found only in chemical reactions that consist of many elementary reactions.[23,24]

Such "OFF−OFF−ON" behaviors would expand the scope of not only the availability of fluorescence techniques for routine analysis of metal ions but also unique control of metal ion-promoted electron-transfer reactions. However, stepwise host (probe molecules or ligands)−guest (metal ions) complex formation has yet to be examined in fluorescence sensors for metal ions or metal ion-promoted electron-transfer reactions.

We report herein an "OFF−OFF−ON" switchable fluorescence sensor for metal ions and the metal ion-promoted electron-transfer reduction of O_2 in stepwise complex formation equilibria of 2,3,5,6-tetrakis(2-pyridyl)pyrazine (TPPZ) with metal ions. TPPZ used as a probe molecule and a host ligand in this work has recently been utilized in a variety of molecular wire complexes as a bridging ligand.[25] TPPZ forms a 2:1 complex $[(TPPZ)_2{-}M^{n+}]$ with metal ions at high concentrations of metal ions; this complex is converted to a 1:1 complex $[TPPZ{-}M^{n+}]$ at high concentrations of metal ions. Such stepwise complex formation of TPPZ with metal ions enables "OFF−OFF−ON" switchability in metal ion fluorescence sensors and metal ion-promoted electron-transfer reactions.

(6) A part of the preliminary results on the fluorescence sensor for Sc^{3+} and Zn^{2+} has appeared. See: Yuasa, J.; Fukuzumi, S. *J. Am. Chem. Soc.* **2006**, *128*, 15976.
(7) Frederickson, C. J.; Klitenick, M. A.; Manton, W. I.; Kirkpatrick, J. B. *Brain Res.* **1983**, *273*, 335.
(8) For "ON−OFF" fluorescence sensors using sequential binding to metal ions, see: (a) Baxter, P. N. W. *Chem.−Eur. J.* **2002**, *8*, 5250. (b) Baxter, P. N. W. *Chem.−Eur. J.* **2003**, *9*, 2531. (c) Baxter, P. N. W. *Chem.−Eur. J.* **2003**, *9*, 5011.
(9) A series of fluorescence sensor molecules with distinct affinities for Zn^{2+} have been applied to fluoresce assays for Zn^{2+}. See: Komatsu, K.; Kikuchi, K.; Kojima, H.; Urano, Y.; Nagano, T. *J. Am. Chem. Soc.* **2005**, *127*, 10197.
(10) For the complex between organic radical anions and transition metals, see: (a) Wanner, M.; Sixt, T.; Klinkhammer, K.-W.; Kaim, W. *Inorg. Chem.* **1999**, *38*, 2753. (b) Schwederski, B.; Kasack, V.; Kaim, W.; Roth, E.; Jordanov, J. *Angew. Chem., Int. Ed. Engl.* **1990**, *29*, 78. (c) Ernst, S.; Hänel, P.; Jordanov, J.; Kaim, W.; Kasack, V.; Roth, E. *J. Am. Chem. Soc.* **1989**, *111*, 1733. (d) Ghumaan, S.; Sarkar, B.; Patra, S.; van Slageren, J.; Fiedler, J.; Kaim, W.; Lahiri, G. K. *Inorg. Chem.* **2005**, *44*, 3210.
(11) For X-ray crystallography of contact and separated ion pairs of alkali metal salts of radical anions, see: (a) Lü, J.-M.; Rosokha, S. V.; Lindeman, S. V.; Neretin, I. S.; Kochi, J. K. *J. Am. Chem. Soc.* **2005**, *127*, 1797. (b) Davlieva, M. G.; Lü, J.-M.; Lindeman, S. V.; Kochi, J. K. *J. Am. Chem. Soc.* **2004**, *126*, 4557. (c) Lü, J.-M.; Rosokha, S. V.; Neretin, I. S.; Kochi, J. K. *J. Am. Chem. Soc.* **2006**, *128*, 16708.
(12) Wu, H.; Zhang, D.; Su, L.; Ohkubo, K.; Zhang, C.; Yin, S.; Mao, L.; Shuai, Z.; Fukuzumi, S.; Zhu, D. *J. Am. Chem. Soc.* **2007**, *129*, 6839.
(13) (a) Fukuzumi, S. *Bull. Chem. Soc. Jpn.* **1997**, *70*, 1. (b) Fukuzumi, S. In *Electron Transfer in Chemistry*; Balzani, V., Ed.; Wiley-VCH: Weinheim, Germany, 2001; Vol. 4, pp 3−67. (c) Fukuzumi, S. *Org. Biomol. Chem.* **2003**, *1*, 609.
(14) (a) Fukuzumi, S.; Nishizawa, N.; Tanaka, T. *J. Chem. Soc., Perkin Trans. 2* **1985**, 371. (b) Fukuzumi, S.; Okamoto, T. *J. Am. Chem. Soc.* **1993**, *115*, 11600.
(15) (a) Itoh, S.; Kawakami, H.; Fukuzumi, S. *J. Am. Chem. Soc.* **1998**, *120*, 7271. (b) Itoh, S.; Kawakami, H.; Fukuzumi, S. *J. Am. Chem. Soc.* **1997**, *119*, 439. (c) Itoh, S.; Kawakami, H.; Fukuzumi, S. *Biochemistry* **1998**, *37*, 6562.
(16) (a) Fukuzumi, S.; Tanaka, T. In *Photoinduced Electron Transfer*; Fox, M. A., Chanon, M., Eds.; Elsevier: Amsterdam, 1988; Part C, Chapter 11, pp 636−687. (b) Fukuzumi, S.; Okamoto, T.; Otera, J. *J. Am. Chem. Soc.* **1994**, *116*, 5503. (c) Fukuzumi, S.; Itoh, S. In *Advances in Photochemistry*; Neckers, D. C., Volman, D. H., von Bünau, G., Eds.; Wiley: New York, 1998; Vol. 25, pp 107−172.
(17) Yuasa, J.; Suenobu, T.; Fukuzumi, S. *ChemPhysChem* **2006**, *7*, 942.
(18) Ohkubo, K.; Menon, S. C.; Orita, A.; Otera, J.; Fukuzumi, S. *J. Org. Chem.* **2003**, *68*, 4720.
(19) We have previously reported that the Lewis acidity of scandium ion (Sc^{3+}) increases with decreasing the nucleophilicity of the counteranion, leading to increase the rate constant of the Sc^{3+}-promoted electron-transfer reaction. See: (a) Yuasa, J.; Suenobu, T.; Ohkubo, K.; Fukuzumi, S. *Chem. Commun.* **2003**, 1070. (b) Fukuzumi, S.; Yuasa, J.; Suenobu, T. *J. Am. Chem. Soc.* **2002**, *124*, 12566.
(20) Tributsch, H.; Pohlmann, L. *Science* **1998**, *279*, 1891.
(21) Okamoto, K.; Fukuzumi, S. *J. Am. Chem. Soc.* **2003**, *125*, 12416.
(22) We have previously reported unusually high kinetic order in the scandium ion (Sc^{3+})-promoted electron-transfer reduction of *p*-benzoquinone (Q) due to the formation of π-dimer radical anion complexes of Q bridged by two and three Sc^{3+} $[Q^{\bullet-}{-}(Sc^{3+})_n{-}Q, n = 2, 3]$. See: Yuasa, J.; Suenobu, T.; Fukuzumi, S. *J. Am. Chem. Soc.* **2003**, *125*, 12090.
(23) (a) Fokin, A. A.; Schreiner, P. R.; Gunchenko, P. A.; Peleshanko, S. A.; Shubina, T. E.; Isaev, S. D.; Tarasenko, P. V.; Kulik, N. I.; Schiebel, H.-M.; Yurchenko, A. G. *J. Am. Chem. Soc.* **2000**, *122*, 7317. (b) Fokin, A. A.; Shubina, T. E.; Gunchenko, P. A.; Isaev, S. D.; Yurchenko, A. G.; Schreiner, P. R. *J. Am. Chem. Soc.* **2002**, *124*, 10718.
(24) (a) Marchaj, A.; Bakac, A.; Espenson, J. H. *Inorg. Chem.* **1992**, *31*, 4860. (b) Bonner, T. G.; Hancock, R. A.; Rolle, F. R.; Yousif, G. *J. Chem. Soc. B* **1970**, 314.
(25) (a) Carlson, C. N.; Kuehl, C. J.; Da Re, R. E.; Veauthier, J. M.; Schelter, E. J.; Milligan, A. E.; Scott, B. L.; Bauer, E. D.; Thompson, J. D.; Morris, D. E.; John, K. D. *J. Am. Chem. Soc.* **2006**, *128*, 7230. (b) Fantacci, S.; De Angelis, F.; Wang, J.; Bernhard, S.; Selloni, A. *J. Am. Chem. Soc.* **2004**, *126*, 9715. (c) Flores-Torres, S.; Hutchison, G. R.; Soltzberg, L. J.; Abruña, H. D. *J. Am. Chem. Soc.* **2006**, *128*, 1513.

Experimental Section

Materials. Scandium triflate [$Sc(OTf)_3$] (OTf = OSO_2CF_3), yttrium triflate [$Y(OTf)_3$], holmium triflate [$Ho(OTf)_3$], neodymium triflate [$Nd(OTf)_3$], europium triflate [$Eu(OTf)_3$], lutetium triflate [$Lu(OTf)_3$], zinc triflate [$Zn(OTf)_2$], strontium perchlorate [$Sr(ClO_4)_2$], and TPPZ were obtained from Aldrich. Magnesium perchlorate [$Mg(ClO_4)_2$], barium perchlorate [$Ba(ClO_4)_2$], lithium perchlorate [$Li(ClO_4)$], and calcium perchlorate [$Ca(ClO_4)_2$] were obtained from Nacalai Tesque. Cobalt(II) tetraphenylporphyrin (CoTPP) was prepared according to the literature.[26] Acetonitrile (MeCN) used as a solvent was purified and dried by the standard procedure.[27] [$^2H_3$]Acetonitrile (CD_3CN) was obtained from EURI SO-TOP, CEA, France.

Spectral Measurements. Formation of metal ion complexes of TPPZ, $(TPPZ)_2-M^{n+}$ and $TPPZ-M^{n+}$, was examined from the UV−vis spectral change of TPPZ in the presence of various concentrations of M^{n+} by using a Hewlett Packard 8453 diode array spectrophotometer. Formation of the $TPPZ-M^{n+}$ complexes was also examined from the fluorescence spectral change of TPPZ in the presence of various concentrations of M^{n+} by a Shimadzu spectrofluorophotometer (RF-5000). The monitoring wavelengths were those corresponding to the maxima of the emission bands of the $TPPZ-M^{n+}$ complexes. The formation of $(TPPZ)_2-Zn^{2+}$ and $TPPZ-Zn^{2+}$ complexes was examined by ESI-MS measurements. ESI-MS data were collected on an API 365 triple quadrupole mass spectrometer (PE-Sciex) in positive detection mode, equipped with an ion spray interface. The sprayer was held at a potential of +5.0 kV, and compressed N_2 was employed to assist liquid nebulization.

Kinetic Measurements. Kinetic measurements were performed by using a Shimadzu UV-3100 PC UV−vis−NIR scanning spectrophotometer. Rates of electron transfer from CoTPP (1.4×10^{-6} M) to O_2 (air saturated: 2.6×10^{-3} M) in the presence of Sc^{3+} [$(0-1.2) \times 10^{-3}$ M] and TPPZ (1.6×10^{-4} to 4.8×10^{-4} M) in MeCN at 298 K were monitored by rise and decay of the absorption bands at 434 and 412 nm due to $CoTPP^+$ and CoTPP, respectively. All kinetic measurements were carried out under pseudo-first-order conditions where the concentrations of O_2, Sc^{3+}, and TPPZ were maintained at more than 10-fold excess of the concentrations of CoTPP at 298 K. Pseudo-first-order rate constants were determined by least-square curve fits using a personal computer.

Fluorescence Quantum Yield Determination. The fluorescence quantum yields (ϕ_f) of the $TPPZ-M^{n+}$ complexes were determined in reference to a fluorescence quantum yield of quinine sulfate ($\phi_f = 0.55$) in 0.5 M sulfuric acid.[28] The excitation wavelength was $\lambda = 349$ nm. All ϕ_f values were determined under conditions such that TPPZ certainly forms the $TPPZ-M^{n+}$ complexes in the presence of sufficient concentrations of metal ions.

Theoretical Calculations. Density functional theory (DFT) calculations were performed on an 8CPU workstation (PQS, Quantum Cube QS8-2400C-064). Geometry optimizations were carried out using the Becke3LYP functional and 6-31G** basis set[29] with the restricted Hartree−Fock formalism and as implemented in the Gaussian 03 program revision C.02.

Results and Discussion

Stepwise Complex Formation of TPPZ with Metal Ions. Upon addition of 0−0.5 equiv of scandium triflate [$Sc(OTf)_3$] (OTf = OSO_2CF_3) [$(0-2.8) \times 10^{-5}$ M] to an MeCN solution of TPPZ (5.7×10^{-5} M), UV−vis spectral changes of TPPZ were observed with isosbestic points at 262, 276, 302, and 311 nm (Figure 1a).[6] Such spectral changes of TPPZ in the presence of 0−0.5 equiv of Sc^{3+} are ascribed to a 2:1 complex formation of TPPZ with Sc^{3+} [$(TPPZ)_2-Sc^{3+}$] (the first step of eq 1).

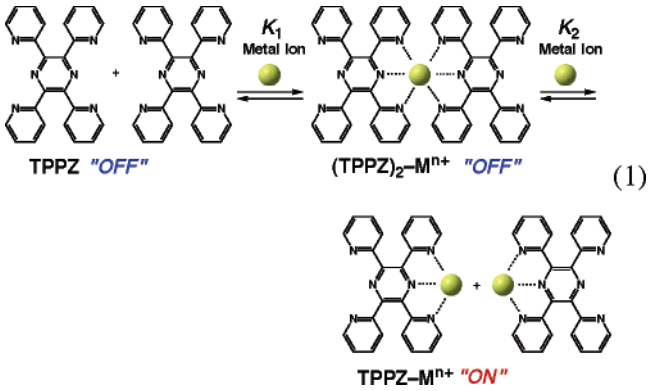

(1)

The plot of $\Delta Abs/\Delta Abs_\infty$ at $\lambda = 358$ nm vs $[Sc^{3+}]/[TPPZ]_0$ (inset of Figure 1a) confirms the stoichiometry of $(TPPZ)_2-Sc^{3+}$ in the first step of eq 1. The absorption spectrum due to $(TPPZ)_2-Sc^{3+}$ (Figures 1a and 2a, blue lines) is further changed by the presence of 0.5−1.0 equiv of Sc^{3+} with isosbestic points at 237 and 278 nm (Figure 2a).[6] Such stepwise UV−vis spectral changes are ascribed to the conversion of the 2:1 complex [$(TPPZ)_2-Sc^{3+}$] to a 1:1 complex of TPPZ with Sc^{3+} ($TPPZ-Sc^{3+}$) (the second step of eq 1). The stoichiometry of the $TPPZ-Sc^{3+}$ complex in the second step of eq 1 is confirmed by the plot of $\Delta Abs/\Delta Abs_\infty$ at $\lambda = 303$ nm vs $[Sc^{3+}]/[TPPZ]_0$ (inset of Figure 2a). TPPZ also shows stepwise UV−vis spectral changes, when the other metal ions (M^{n+}: Y^{3+}, Ho^{3+}, Eu^{3+}, Lu^{3+}, Nd^{3+}, Zn^{2+}, Mg^{2+}, Ca^{2+}, Ba^{2+}, Sr^{2+}, and Li^+) are employed instead of Sc^{3+} (Figures 1b−d and 2b−d; Figures S1 and S2 in Supporting Information). This indicates that TPPZ forms the 2:1 complexes [$(TPPZ)_2-M^{n+}$] with a series of metal ions, which are converted to the 1:1 complexes ($TPPZ-M^{n+}$) at high concentrations of metal ions (eq 1).[30] In the case of Sc^{3+}, which acts as the strongest Lewis acid among a series of metal ions, $TPPZ-Sc^{3+}$ is further converted to $TPPZ-(Sc^{3+})_2$ at high concentration range of Sc^{3+} (8.0×10^{-4} to 1.6×10^{-2} M), and the $TPPZ-(Sc^{3+})_2$ complex fluoresces as strong as $TPPZ-Sc^{3+}$ (see Supporting Information S3).[31]

Formation of the $(TPPZ)_2-M^{n+}$ and $TPPZ-M^{n+}$ complexes was also examined by ESI-MS measurements in stepwise complex formation of TPPZ with Zn^{2+} in MeCN.[6,32] The positive-ion ESI mass spectrum of TPPZ (3.9×10^{-5} M) in MeCN in the presence of low (3.0×10^{-5} M; Figure 3a) and high (6.8×10^{-5} M; Figure 3c) concentrations of Zn^{2+} shows signals at m/z +989.3 and at +601.1 m/z, which correspond to $\{[Zn(TPPZ)_2](OSO_2CF_3)\}^+$ and $\{[Zn(TPPZ)](OSO_2CF_3)\}^+$, re-

(26) Shirazi, A.; Goff, H. M. *Inorg. Chem.* **1982**, *21*, 3420.
(27) Armarego, W. L. F.; Chai, C. L. L. *Purification of Laboratory Chemicals*, 5th ed.; Butterworth-Heinemann: Amsterdam, 2003.
(28) Crosby, G. A.; Demas, J. N. *J. Phys. Chem.* **1971**, *75*, 991.
(29) Becke, A. D. *J. Chem. Phys.* **1993**, *98*, 5648.
(30) We have also examined complex formation of TPPZ with the potentially interfering metal ion such as Fe(II). TPPZ also forms the complex with Fe(II) in MeCN. However, the Fe(II) complex of TPPZ exhibits no fluorescence. For the Fe(II) complex of TPPZ, see: Campos-Fernández, C. S.; Smucker, B. W.; Clérac, R.; Dunbar, K. R. *Isr. J. Chem.* **2001**, *41*, 207.
(31) The Lewis acidities of the other metal ions are not strong enough to form the 1:2 complexes [$TPPZ-(M^{n+})_2$].
(32) Formation of $(TPPZ)_2-Sc^{3+}$ and $TPPZ-Sc^{3+}$ is confirmed by ^1H NMR. The ^1H NMR signals of TPPZ exhibit a downfield shift in the presence of 0.5 equiv of Sc^{3+}, demonstrating development of positive charge by formation of $(TPPZ)_2-Sc^{3+}$. The ^1H NMR signals of $(TPPZ)_2-Sc^{3+}$ exhibit a further downfield shift in the presence of 1 equiv of Sc^{3+} due to the additional binding of Sc^{3+} to yield the 1:1 complex, $TPPZ-Sc^{3+}$. However, $(TPPZ)_2-Sc^{3+}$ and $TPPZ-Sc^{3+}$ could not be detected by positive-ion ESI mass spectrum, which may be due to multivalency of the Sc^{3+} complex of TPPZ.

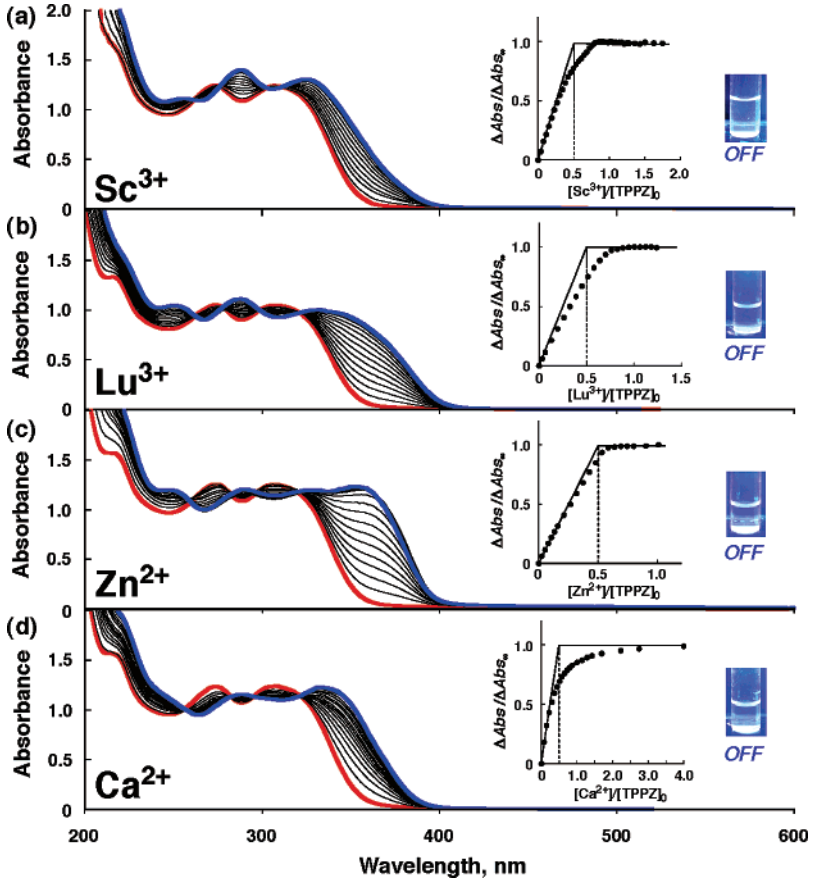

Figure 1. UV−vis absorption spectra of (a) TPPZ (5.7×10^{-5} M) in the presence of Sc^{3+} [0 M (red line) to 2.8×10^{-5} M (blue line)], (b) TPPZ (4.9×10^{-5} M) in the presence of Lu^{3+} [0 M (red line) to 4.0×10^{-5} M (blue line)], (c) TPPZ (5.7×10^{-5} M) in the presence of Zn^{2+} [0 M (red line) to 3.0×10^{-5} M (blue line)], and (d) TPPZ (5.8×10^{-5} M) in the presence of Ca^{2+} [0 M (red line) to 2.0×10^{-4} M (blue line)] in MeCN at 298 K. Insets: Plots of $\Delta Abs/\Delta Abs_\infty$ (a) at $\lambda = 358$ nm vs $[Sc^{3+}]/[TPPZ]_0$, (b) at 360 nm vs $[Lu^{3+}]/[TPPZ]_0$, (c) at $\lambda = 355$ nm vs $[Zn^{2+}]/[TPPZ]_0$, and (d) at $\lambda = 355$ nm vs $[Ca^{2+}]/[TPPZ]_0$. Photographs of MeCN solutions of TPPZ (2.0×10^{-2} M) in the presence of (a) Sc^{3+} (1.0×10^{-2} M), (b) Lu^{3+} (1.0×10^{-2} M), (c) Zn^{2+} (1.0×10^{-2} M), and (d) Ca^{2+} (1.0×10^{-2} M) under UV light irradiation.

spectively.[33] Those signals have a characteristic distribution of isotopomers (Figure 3a,c) that matches well with the calculated isotopic distribution for $\{[Zn(TPPZ)_2](OSO_2CF_3)\}^+$ and $\{[Zn(TPPZ)](OSO_2CF_3)\}^+$ as shown in Figure 3b,d, respectively.

The visible fluorescence photographs of TPPZ in the presence of 0.5 and more than 1 equiv of metal ions (Sc^{3+}, Lu^{3+}, Zn^{2+}, and Ca^{2+}) are shown in the insets of Figures 1 and 2, respectively. The 1:1 complexes ($TPPZ-M^{n+}$) exhibit strong fluorescence (insets of Figure 2). Since TPPZ itself hardly fluoresces, the fluorescence of the $TPPZ-M^{n+}$ complexes may result from the change in the lowest excited state from the n,π* triplet to the π,π* singlet, which becomes lower in energy than the n,π* triplet due to the complexation with M^{n+} acting as a strong Lewis acid.[34−36] In contrast, the $(TPPZ)_2-M^{n+}$ complexes hardly fluoresce (insets of Figure 1). The strong binding of M^{n+} in the $TPPZ-M^{n+}$ complexes may be significantly weakened in the 2:1 complex $[(TPPZ)_2-M^{n+}]$, in which the lowest excited state may still be the n,π* triplet.[37]

The fluorescence spectral titration of TPPZ by M^{n+} was examined under the same experimental conditions as employed for the UV−vis spectral titration (Figures 1 and 2). The results are shown in Figure 4. Typically, TPPZ shows stepwise fluorescence spectral changes in response to $[Sc^{3+}]/[TPPZ]_0$ at 0−0.5 (red and blue lines) and 0.5−1.0 (blue and green lines) (Figure 4a) as in the case of the UV−vis spectral titration of TPPZ by Sc^{3+} (Figures 1a and 2a).[6] Such stepwise fluorescence spectral changes are also ascribed to stepwise complex formation between TPPZ and Sc^{3+} (eq 1). The fluorescence intensity (F. L. intensity) at $\lambda = 453$ nm (inset of Figure 4a) due to the $TPPZ-Sc^{3+}$ complex is plotted against $[Sc^{3+}]/[TPPZ]_0$, where fluorescence intensity starts to increase at Sc^{3+} concentrations above the 1:2 ratio ($[Sc^{3+}]/[TPPZ]_0 > 0.5$). TPPZ also shows stepwise fluorescence changes in the fluorescence spectral titration of TPPZ by the other metal ions (Figure 4b−d; Figure S5 in Supporting Information). There is very weak fluorescence due to the $(TPPZ)_2-M^{n+}$ complexes at low concentrations of metal ions (Figures 4 and S5, blue lines). However, strong

(33) The crystal structure of the $TPPZ-Zn^{2+}$ complex has been previously reported. See: Graf, M.; Greaves, B.; Stoeckli-Evans, H. S. *Inorg. Chim. Acta* **1993**, *204*, 239.
(34) Lewis, F. D.; Reddy, G. D.; Elbert, J. E.; Tillberg, B. E.; Meltzer, J. A.; Kojima, M. *J. Org. Chem.* **1991**, *56*, 5311.
(35) Fukuzumi, S.; Satoh, N.; Okamoto, T.; Yasui, K.; Suenobu, T.; Seko, Y.; Fujitsuka, M.; Ito, O. *J. Am. Chem. Soc.* **2001**, *123*, 7756.
(36) The partial structure fixation of TPPZ by complex formation with M^{n+} ($TPPZ-M^{n+}$) may also be ascribed to strong fluorescence of $TPPZ-M^{n+}$, where the rotation of coordinated pyridine rings is restricted. This rotation may be less restricted in the 2:1 complexes $[TPPZ-(M^{n+})_2]$ because of the weaker binding of M^{n+} in the $TPPZ-(M^{n+})_2$ complexes than that in the $TPPZ-M^{n+}$ complexes.
(37) The optimized structures of $TPPZ-Mg^{2+}$ and $(TPPZ)_2-Mg^{2+}$ obtained by using DFT at the B3LYP/6-31G** basis support the stronger binding of Mg^{2+} in the 1:1 complex ($TPPZ-Mg^{2+}$) than that in the 2:1 complex $[(TPPZ)_2-Mg^{2+}]$, in which the bond length between Mg^{2+} and the pyrazine nitrogen in the $(TPPZ)_2-Mg^{2+}$ complex (2.17 Å) becomes shorter (2.01 Å) in the $TPPZ-Mg^{2+}$ complex (see Supporting Information S4).

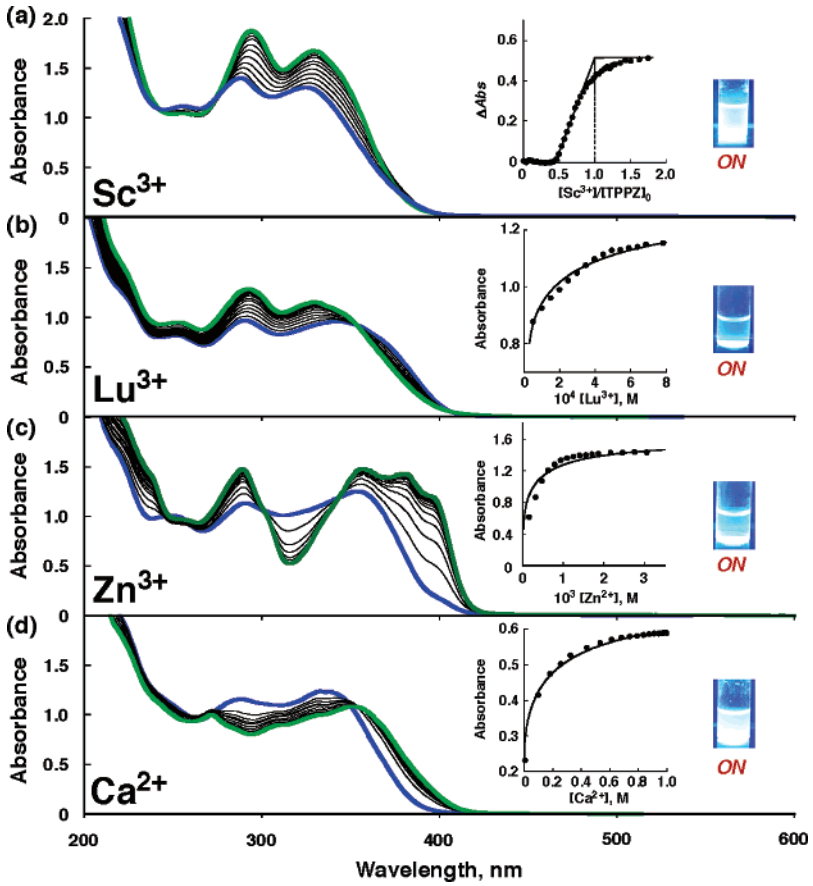

Figure 2. UV−vis absorption spectra of (a) TPPZ (5.7×10^{-5} M) in the presence of Sc^{3+} [2.8×10^{-5} M (blue line) to 5.9×10^{-5} M (green line)], (b) TPPZ (4.9×10^{-5} M) in the presence of Lu^{3+} [1.0×10^{-4} M (blue line) to 1.0×10^{-3} M (green line)], (c) TPPZ (5.7×10^{-5} M) in the presence of Zn^{2+} [3.0×10^{-5} M (blue line) to 3.1×10^{-3} M (green line)], and (d) TPPZ (5.8×10^{-5} M) in the presence of Ca^{2+} [5.1×10^{-3} M (blue line) to 7.9×10^{-1} M (green line)] in MeCN at 298 K. Insets: Plots of (a) ΔAbs at $\lambda = 303$ nm vs $[Sc^{3+}]/[TPPZ]_0$, (b) absorbance at 330 nm vs $[Lu^{3+}]$, (c) absorbance at 381 nm vs $[Zn^{2+}]$, and (d) absorbance at 380 nm vs $[Ca^{2+}]$. Photographs of MeCN solutions of TPPZ (2.0×10^{-2} M) in the presence of (a) Sc^{3+} (2.0×10^{-2} M), (b) Lu^{3+} (7.0×10^{-2} M), (c) Zn^{2+} (2.0×10^{-2} M), and (d) Ca^{2+} (2.0×10^{-2} M) under UV light irradiation.

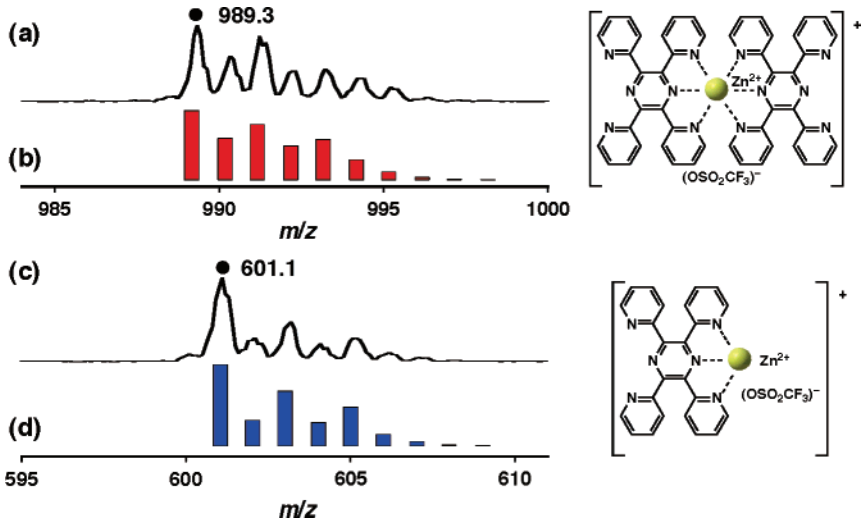

Figure 3. Positive-ion ESI mass spectra of an MeCN solution of TPPZ (3.9×10^{-5} M) in the presence of Zn^{2+} [(a) 3.0×10^{-5} M and (c) 6.8×10^{-5} M]. The signals at (a) *m*/*z* 989.3 and (c) *m*/*z* 601.1 correspond to $\{[Zn(TPPZ)_2](OSO_2CF_3)\}^+$ and $\{[Zn(TPPZ)](OSO_2CF_3)\}^+$, respectively. Calculated isotopic distributions are shown for (b) $\{[Zn(TPPZ)_2](OSO_2CF_3)\}^+$ and (d) $\{[Zn(TPPZ)](OSO_2CF_3)\}^+$.

fluorescence starts to appear at $\lambda = 453$ nm (Lu^{3+}), $\lambda = 432$ nm (Zn^{2+}), and $\lambda = 429$ nm (Ca^{2+}) (Figure 4, green lines) at high concentrations of metal ions, which are ascribed to formation of the TPPZ−M^{n+} complexes (see Supporting Information S5).

Normalized absorbance for the titration of TPPZ by M^{n+} at low concentrations of M^{n+} is plotted against logarithm of M^{n+} concentrations ($\log[M^{n+}]$) (Figure 5a), which corresponds to the 2:1 complex formation of TPPZ with M^{n+}. In the case of trivalent metal ions (Sc^{3+}, Y^{3+}, Ho^{3+}, Eu^{3+}, Lu^{3+}, and Nd^{3+})

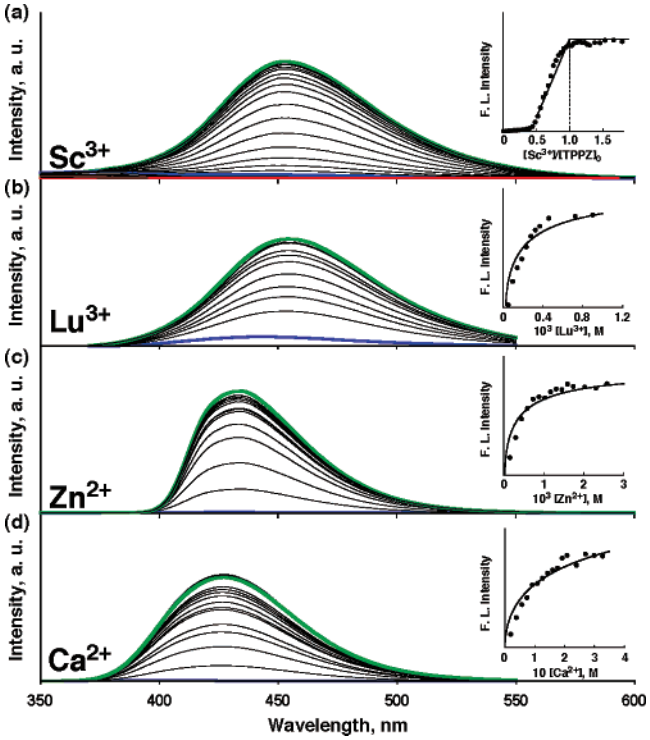

Figure 4. Fluorescence spectra of (a) TPPZ (5.7×10^{-5} M) in the presence of Sc^{3+} [0 M (red line) to 2.8×10^{-5} M (blue line) to 5.9×10^{-5} M (green line)], (b) TPPZ (4.9×10^{-5} M) in the presence of Lu^{3+} [4.6×10^{-5} M (blue line) to 9.0×10^{-4} M (green line)], (c) TPPZ (5.7×10^{-5} M) in the presence of Zn^{2+} [3.0×10^{-5} M (blue line) to 3.1×10^{-3} M (green line)], and (d) TPPZ (5.8×10^{-5} M) in the presence of Ca^{2+} [6.7×10^{-4} M (blue line) to 3.5×10^{-1} M (green line)] in MeCN at 298 K. The excitation wavelengths were (a) $\lambda = 315$ nm, (b) $\lambda = 355$ nm, (c) $\lambda = 343$ nm, and (d) $\lambda = 324$ nm. Insets: Plots of fluorescence intensity (a) at $\lambda = 453$ nm vs $[Sc^{3+}]/[TPPZ]_0$, (b) at $\lambda = 453$ nm vs $[Lu^{3+}]$, (c) at $\lambda = 432$ nm vs $[Zn^{2+}]$, and (d) at $\lambda = 429$ nm vs $[Ca^{2+}]$.

and Zn^{2+}, Mg^{2+}, and Ca^{2+}, acting as strong Lewis acids, those metal ions form the 2:1 complex $[(TPPZ)_2{-}M^{n+}]$ almost stoichiometrically with TPPZ (Figure 5a, closed circles). In such a case, the formation constants (K_1) of the $(TPPZ)_2{-}M^{n+}$ complexes can be determined by using eq 2, where A is absorbance of TPPZ in the presence of M^{n+}, $\alpha = (A - A_0)(A_\infty - A_0)^{-1}$, and A_0 and A_∞ are absorbance due to TPPZ and $(TPPZ)_2{-}M^{n+}$, respectively (for derivation of eq 2, see Supporting Information S6).[38]

$$(1 - \alpha)^{-2} = K_1[\mathrm{TPPZ}]_0(2[\mathrm{M}^{n+}]\alpha^{-1} - [\mathrm{TPPZ}]_0) \quad (2)$$

The linear plots of $(1 - \alpha)^{-2}$ vs $[M^{n+}]\alpha^{-1}$ are obtained. The K_1 values are $(1.4 \pm 0.1) \times 10^{10}$ M^{-2} (Ho^{3+}), $(2.4 \pm 0.3) \times 10^{10}$ M^{-2} (Eu^{3+}), $(2.3 \pm 0.2) \times 10^{10}$ M^{-2} (Lu^{3+}), $(5.9 \pm 1.3) \times 10^{10}$ M^{-2} (Nd^{3+}), $(2.3 \pm 0.1) \times 10^{9}$ M^{-2} (Mg^{2+}), and $(5.2 \pm 0.4) \times 10^{9}$ M^{-2} (Ca^{2+}) (see Supporting Information S7).[39] In contrast, the other metal ions (Ba^{2+}, Sr^{2+}, and Li^{+}) acting as weak Lewis acids form the $(TPPZ)_2{-}M^{n+}$ complexes in the presence of much more than 0.5 equiv of metal ions (Figure 5a, closed triangles). In such a case, the absorbance change ($A - A_0 = \Delta Abs$) due to formation of the $TPPZ{-}M^{n+}$ complex is expressed by eq 3 (for derivation of eq 3, see Supporting Information S8).

$$(A - A_0) = (A_\infty - A_0) \times \frac{4K_1[\mathrm{M}^{n+}][\mathrm{TPPZ}]_0 + 1 - \sqrt{8K_1[\mathrm{M}^{n+}][\mathrm{TPPZ}]_0 + 1}}{4K_1[\mathrm{M}^{n+}][\mathrm{TPPZ}]_0} \quad (3)$$

The K_1 values of $TPPZ{-}M^{n+}$ are determined as $(1.2 \pm 0.1) \times 10^7$ M^{-2} (Ba^{2+}), $(7.5 \pm 0.4) \times 10^7$ M^{-2} (Sr^{2+}), and $(3.1 \pm 0.1) \times 10^6$ M^{-2} (Li^{+}) from the best-fit lines for the dependence of ΔAbs on $[M^{n+}]$ (Figure S1).

Plots of normalized absorbance and fluorescence intensity due to $TPPZ{-}M^{n+}$ vs log $[M^{n+}]$ for the titration of TPPZ by M^{n+} at high concentrations of M^{n+} are shown in Figure 5b,c, respectively. The dependence of normalized fluorescence intensity due to $TPPZ{-}M^{n+}$ on $\log[M^{n+}]$ (Figure 5c) agrees with that of normalized absorbance on log $[M^{n+}]$ (Figure 5b). Such absorbance and fluorescence intensity changes due to formation of the $TPPZ{-}M^{n+}$ complex are expressed by eq 4, where A is absorbance of TPPZ in the presence of M^{n+} ($2[M^{n+}] > [TPPZ]_0$), and A_0 and A_∞ are absorbance due to $(TPPZ)_2{-}M^{n+}$ and $TPPZ{-}M^{n+}$, respectively (for derivation of eq 4, see Supporting Information S9).

$$(A - A_0) = (A_\infty - A_0) \times \quad (\text{or } I) \qquad (\text{or } I_\infty)$$
$$\frac{-K_2[\mathrm{M}^{n+}] + \sqrt{K_2{}^2[\mathrm{M}^{n+}]^2 + (4 - K_2)K_2[\mathrm{TPPZ}]_0(2[\mathrm{M}^{n+}] - [\mathrm{TPPZ}]_0)}}{(4 - K_2)[\mathrm{TPPZ}]_0} \quad (4)$$

The formation constants (K_2) of the $TPPZ{-}M^{n+}$ complex are determined from the best-fit lines in insets of Figures 2 and S2, where the K_2 values vary from $(1.4 \pm 0.1) \times 10^2$ (Sc^{3+}) to $(4.4 \pm 1.3) \times 10^{-5}$ (Ba^{2+}). The K_1 and K_2 values are listed in Table 1 together with the absorption maxima of $(TPPZ)_2{-}M^{n+}$ (λ_1) and $TPPZ{-}M^{n+}$ (λ_2), emission maxima (λ_e), excitation energies ($\Delta E_{0,0}$), and the fluorescence quantum yields (ϕ_f) of the $TPPZ{-}M^{n+}$ complexes.[40] We have previously derived the binding energies (ΔE) of superoxide–metal ion complexes ($O_2^{\bullet-}{-}M^{n+}$) from the g_{zz} values of ESR spectra of $O_2^{\bullet-}{-}M^{n+}$ complexes, which are highly sensitive to the Lewis acidity of a series of metal ions and provide a quantitative measure of Lewis acidity of metal ions.[42] Linear correlations are observed in plots of log K_1 and log K_2 vs ΔE (Figure 6, open and closed circles, respectively). This indicates that the binding strength of metal ion with TPPZ in $(TPPZ)_2{-}M^{n+}$ and $TPPZ{-}M^{n+}$ is mainly determined by the Lewis acidity of metal ions. Some deviations in the linear plots of log K_1 and log K_2 vs ΔE indicate that the counteranions of metal ions may also affect the binding constants

(38) Absorbance of TPPZ in the presence of M^{n+} (A) is derived from the sum of absorbance due to TPPZ and $(TPPZ)_2{-}M^{n+}$ at any wavelength, which can be expressed by eq 2 (see derivation of eq 2 in Supporting Information S6).

(39) In the case of Sc^{3+}, Y^{3+}, and Zn^{2+}, the K_1 values are too large to be determined actually.

(40) Absorption maxima, fluorescence maxima, and fluorescence quantum yields of $TPPZ{-}M^{n+}$ were determined in the presence of sufficient concentrations of metal ions such that TPPZ certainly forms the 1:1 complexes ($TPPZ{-}M^{n+}$). In the case of $TPPZ{-}Li^{+}$, however, only 53% of TPPZ forms the $TPPZ{-}Li^{+}$ complex even in the presence of 8.1×10^{-1} M of Li^{+} due to the extremely small binding constant of the $TPPZ{-}Li^{+}$ complex. On the other hand, absorption maxima of the $(TPPZ)_2{-}M^{n+}$ complexes were determined under conditions such that the 2:1 complexes $[(TPPZ)_2{-}M^{n+}]$ are not converted to the 1:1 complexes ($TPPZ{-}M^{n+}$) as shown in Figures 1 and S1.

(41) Shannon, R. D. *Acta Crystallogr.* **1976**, *A32*, 751.
(42) Fukuzumi, S.; Ohkubo, K. *Chem.–Eur. J.* **2000**, *6*, 4532.
(43) Fukuzumi, S.; Ohkubo, K. *J. Am. Chem. Soc.* **2002**, *124*, 10270.

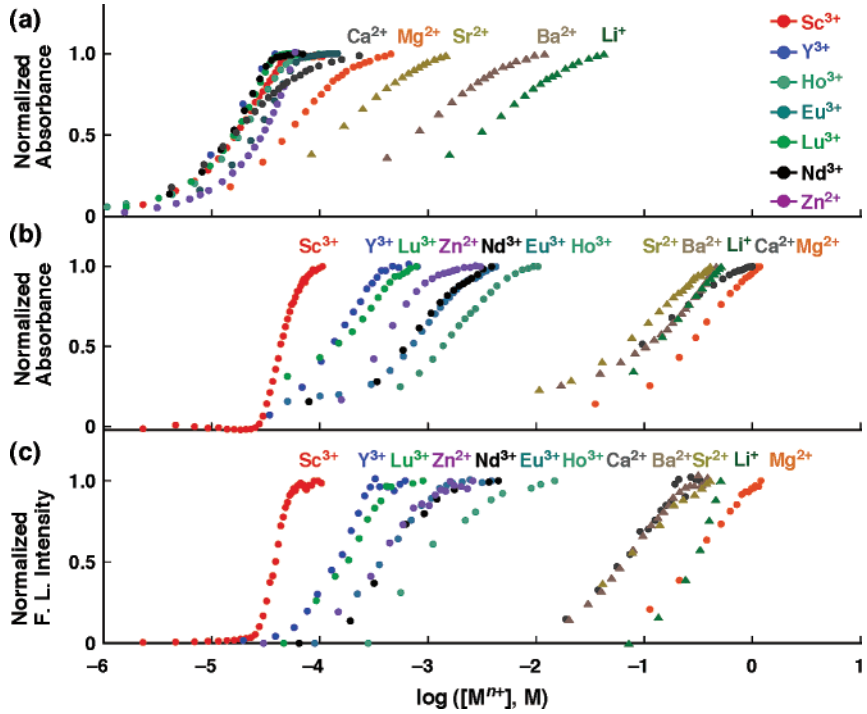

Figure 5. (a) Plots of normalized absorbance vs log [M^{n+}] for the titration of TPPZ by M^{n+} at low concentrations of M^{n+}. Plots of normalized (b) absorbance and (c) fluorescence intensity vs log[M^{n+}] for the titration of TPPZ by M^{n+} at high concentrations of M^{n+}.

Table 1. Ion Radii (r) and Binding Energies (ΔE) of $O_2^{\bullet-}$−Metal Ion Complexes, Formation Constants of $(TPPZ)_2-M^{n+}$ (K_1) and $TPPZ-M^{n+}$ (K_2), Absorption Maxima of $(TPPZ)_2-M^{n+}$ (λ_1) and $TPPZ-M^{n+}$ (λ_2), Emission Maxima of $TPPZ-M^{n+}$ (λ_e), Excitation Energies ($\Delta E_{0,0}$) of $TPPZ-M^{n+}$, and the Fluorescence Quantum Yields (ϕ_f) of $TPPZ-M^{n+}$ in MeCN at 298 K

metal salt	r[a] (Å)	ΔE[b] (eV)	K_1 (M^{-2})	K_2	λ_1 (nm)	λ_2 (nm)	λ_e (nm)	$\Delta E_{0,0}$[g] (eV)	ϕ[h]
absence of metal salt					308[f]				
$Sc(OTf)_3$	0.81	1.00	*d*	$(1.4 \pm 0.1) \times 10^2$	325	331	453	3.16	0.022
$Y(OTf)_3$	1.02	0.85	*d*	$(8.2 \pm 1.4) \times 10^{-1}$	331	330	450	3.18	0.017
$Ho(OTf)_3$	1.02		$(1.4 \pm 0.1) \times 10^{10}$	$(6.0 \pm 0.3) \times 10^{-2}$	345	345	455	3.10	0.011
$Eu(OTf)_3$	1.25	0.82	$(2.4 \pm 0.3) \times 10^{10}$	$(6.0 \pm 0.3) \times 10^{-2}$	353	365	451	3.04	0.006
$Lu(OTf)_3$	0.98	0.83	$(2.3 \pm 0.2) \times 10^{10}$	$(2.7 \pm 0.1) \times 10^{-1}$	332	330	453	3.17	0.029
$Nd(OTf)_3$	1.11		$(5.9 \pm 1.3) \times 10^{10}$	$(2.9 \pm 0.3) \times 10^{-2}$	354	380	439	3.03	0.005
$Zn(OTf)_2$	0.90	0.71[c]	*d*	$(2.1 \pm 0.3) \times 10^{-1}$	352	379	432	3.06	0.19
$Mg(ClO_4)_2$	0.89	0.65	$(2.3 \pm 0.1) \times 10^9$	$(9.5 \pm 5.3) \times 10^{-5}$	344	362	432	3.12	0.26
$Ca(ClO_4)_2$	1.12	0.58	$(5.2 \pm 0.4) \times 10^9$	$(3.7 \pm 0.6) \times 10^{-4}$	330	350	429	3.18	0.19
$Ba(ClO_4)_2$	1.42	0.49	$(1.2 \pm 0.1) \times 10^7$	$(4.4 \pm 1.3) \times 10^{-5}$	328	330	403	3.38	0.069
$Sr(ClO_4)_2$	1.26	0.52	$(7.5 \pm 0.4) \times 10^7$	$(3.7 \pm 0.7) \times 10^{-4}$	330	341	412	3.29	0.14
$Li(ClO_4)$	0.92	0.53	$(3.1 \pm 0.1) \times 10^6$	*e*	330		404		0.018

[a] Effective ion radius (coordination number = 8).[41] [b] Taken from ref 42. [c] Taken from ref 43. [d] Too large to be determined accurately. [e] Too small to be determined accurately. [f] Absorption maxima of TPPZ in the absence of metal salt. [g] Determined from the absorption maxima and emission maxima in MeCN. [h] Quinine sulfate ($\phi_f = 0.55$) in 0.5 M sulfuric acid was used as a reference.

of $(TPPZ)_2-M^{n+}$ and $TPPZ-M^{n+}$.[44] In the case of Zn^{2+}, the binding constant (K_2) of the 1:1 complex ($TPPZ-Zn^{2+}$) is much larger than the other divalent metal ions.[45] In such a case, Zn^{2+} forms the fluorescent $TPPZ-M^{n+}$ complex with TPPZ in water (see Supporting Information S10).

The fluorescence quantum yields of the $TPPZ-M^{n+}$ complexes were determined in a series of metal ions.[6,40] The results are shown in Figure 7, where the fluorescence quantum yields of the divalent metal complexes ($TPPZ-M^{2+}$) are much larger than those of the trivalent metal complexes ($TPPZ-M^{3+}$).[46] The formation constants (K_2) of the $TPPZ-M^{n+}$ complexes may not affect the fluorescence quantum yields, because $TPPZ-Zn^{2+}$, which has virtually the same formation constant as that of $TPPZ-M^{3+}$, has a much larger fluorescence quantum yield ($\phi_f = 0.19$) than that of $TPPZ-M^{3+}$ ($\phi_f = 0.005-0.022$) (Table 1).

Fluorescence Sensor for Metal Ions in a Wide Concentration Range. The availability of such an "OFF−OFF−ON" fluorescence sensor for detection of metal ions in a wide

(44) A series of metal ions with different counteranions are chosen in this work, since the ΔE values of those metal ions have been given in ref 42.

(45) With regard to metal ion selectivity, TPPZ has a much larger K_2 value for Zn^{2+} as compared with other biologically important metal ions such as Mg^{2+} and Ca^{2+} (Table 1). This means that TPPZ forms the fluorescent 1:1 complex ($TPPZ-M^{n+}$) selectively with Zn^{2+} among biologically relevant metal ions.

(46) The fluorescence quantum yields of $TPPZ-M^{n+}$ may be related to the fluorescence maxima of the $TPPZ-M^{n+}$ complexes, because fluorescence lifetimes of the trivalent metal complexes ($TPPZ-Sc^{3+}$ and $TPPZ-Y^{3+}$) that fluoresce at longer wavelength are much shorter than those of divalent metal complexes ($TPPZ-Mg^{2+}$ and $TPPZ-Ca^{2+}$) (see Supporting Information S11).

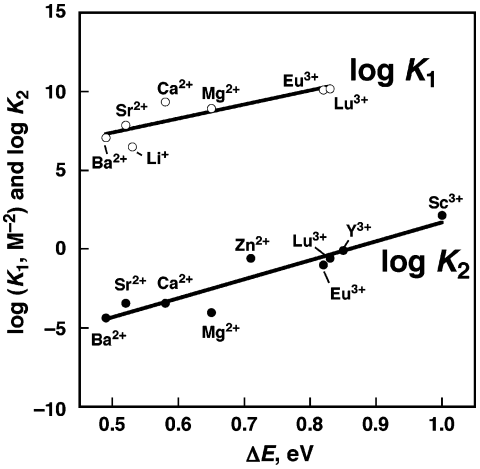

Figure 6. Plots of log K_1 (open circles) and log K_2 (closed circles) vs ΔE.

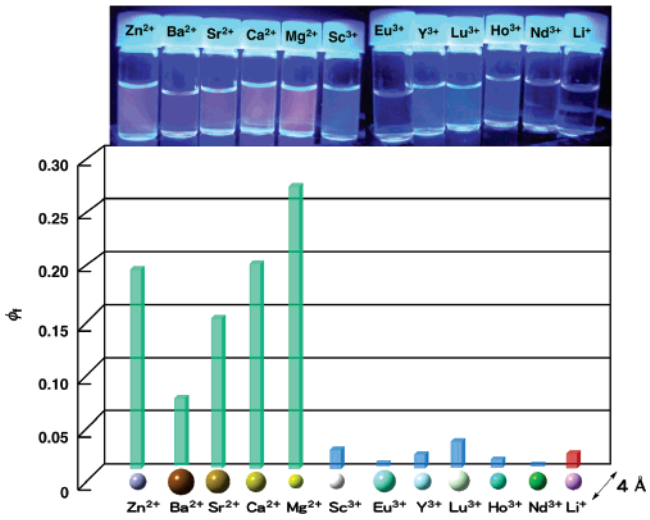

Figure 7. Visible fluorescence and fluorescence quantum yields (ϕ_f) of TPPZ (6.0×10^{-7} M) in the presence of Zn^{2+} (1.1×10^{-2} M); Ba^{2+} (9.9×10^{-1} M); Sr^{2+} (7.4×10^{-1} M); Ca^{2+} (8.8×10^{-1} M); Mg^{2+} (8.2×10^{-1} M); Sc^{3+} (1.2×10^{-2} M); Eu^{3+} (1.1×10^{-2} M); Y^{3+} (6.2×10^{-3} M); Lu^{3+} (4.0×10^{-3} M); Ho^{3+} (3.4×10^{-3} M); Nd^{3+} (2.8×10^{-2} M); and Li^{+} (8.1×10^{-1} M) in MeCN at 298 K.

concentration range is confirmed by fluorescence sensing of Sc^{3+} (vide infra).[47,48] The fluorescence in the presence of various concentrations of TPPZ (1.0×10^{-5} to 5.0×10^{-5} M) and Sc^{3+} [$(0-3.6) \times 10^{-5}$ M] was visualized as shown in Figure 8a.[6] The strong fluorescence due to the TPPZ$-Sc^{3+}$ complex was observed in the presence of more than 0.5 equiv of Sc^{3+} at each concentration of TPPZ.[49] Dependence of the ratio of the fluorescence intensity to the final fluorescence intensity (I/I_∞) on [Sc^{3+}] is shown in Figure 8b, where I/I_∞ starts to increase at

(47) TPPZ also acts as the "OFF−OFF−ON" fluorescence sensor for other metal ions (see insets of Figures 1 and 2).

(48) The detection limit was determined to be 2.0×10^{-6} M in fluorescence sensing of Sc^{3+}, that is, detectable fluorescence was observed in an MeCN solution of TPPZ (1.0×10^{-6} M) in the presence of 2.0×10^{-6} M of Sc^{3+}. Although the detection limit of this system is not completely satisfactory, our concept should be general enough to apply other fluorescence sensors that show stepwise complexation with metal ions. Thus, the detection limit of this system would be improved by using other probe molecules (including derivation of TPPZ) that have high affinities for metal ions.

(49) Formation of TPPZ$-M^{n+}$ and $(TPPZ)_2-M^{n+}$ is also dependent on the concentrations of TPPZ and metal ions. Typically, no sufficient 1:1 complex (TPPZ$-M^{n+}$) is formed in the presence of low concentrations of TPPZ ([TPPZ] $< 1.0 \times 10^{-6}$ M) and metal ions ([M^{n+}] $< 1.0 \times 10^{-6}$ M). This is the detection limit of this system.[48]

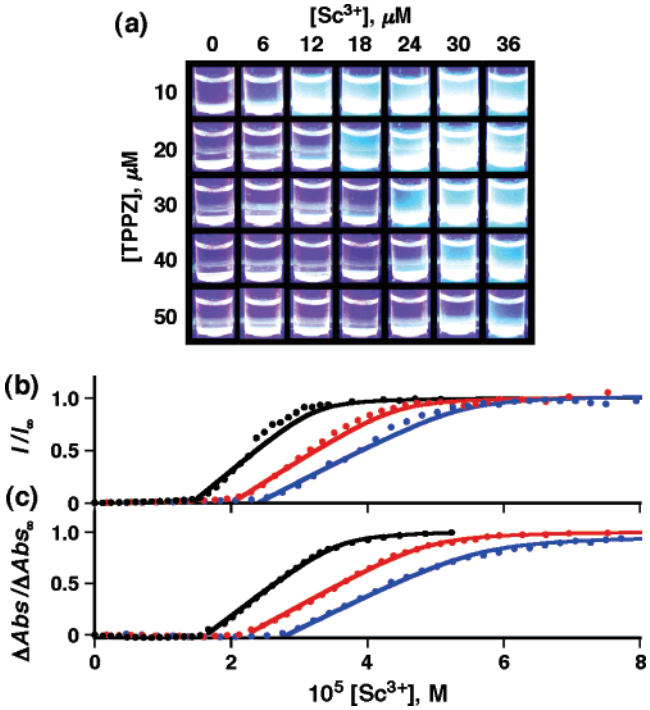

Figure 8. (a) Change in visible fluorescence of MeCN solutions of TPPZ (1.0×10^{-5} to 5.0×10^{-5} M) in the presence of Sc^{3+} [$(0-3.6) \times 10^{-5}$ M]. Plots of (b) I/I_∞ at 453 nm and (c) $\Delta Abs/\Delta Abs_\infty$ [$= (A - A_0)/(A_\infty - A_0)$] at 303 nm vs [$Sc^{3+}$] for the titration of TPPZ [3.4×10^{-5} M (black closed circles), 4.7×10^{-5} M (red closed circles), and 5.7×10^{-5} M (blue closed circles)] by Sc^{3+} in MeCN at 298 K.

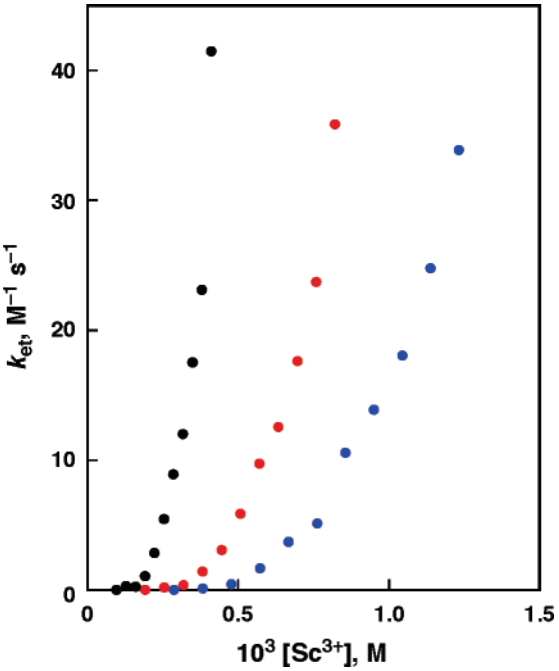

Figure 9. Dependence of k_{et} on [Sc^{3+}] for electron transfer from CoTPP (1.4×10^{-6} M) to O_2 (air saturated, 2.6×10^{-3} M) in the presence of Sc^{3+} and TPPZ [1.6×10^{-4} M (black closed circles), 3.2×10^{-4} M (red closed circles), and 4.8×10^{-4} M (blue closed circles)] in MeCN at 298 K.

Sc^{3+} concentrations above the 1:2 ratio ([Sc^{3+}]/[TPPZ]$_0$ > 0.5), which is shifted to the larger value with increasing the initial concentration of TPPZ [3.4×10^{-5} M (black closed circles), 4.7×10^{-5} M (red closed circles), and 5.7×10^{-5} M (blue closed circles)].[6] The dependence of I/I_∞ on [Sc^{3+}] (Figure 8b) agrees with that of $\Delta Abs/\Delta Abs_\infty$ on [Sc^{3+}] (Figure 8c).

Scheme 3

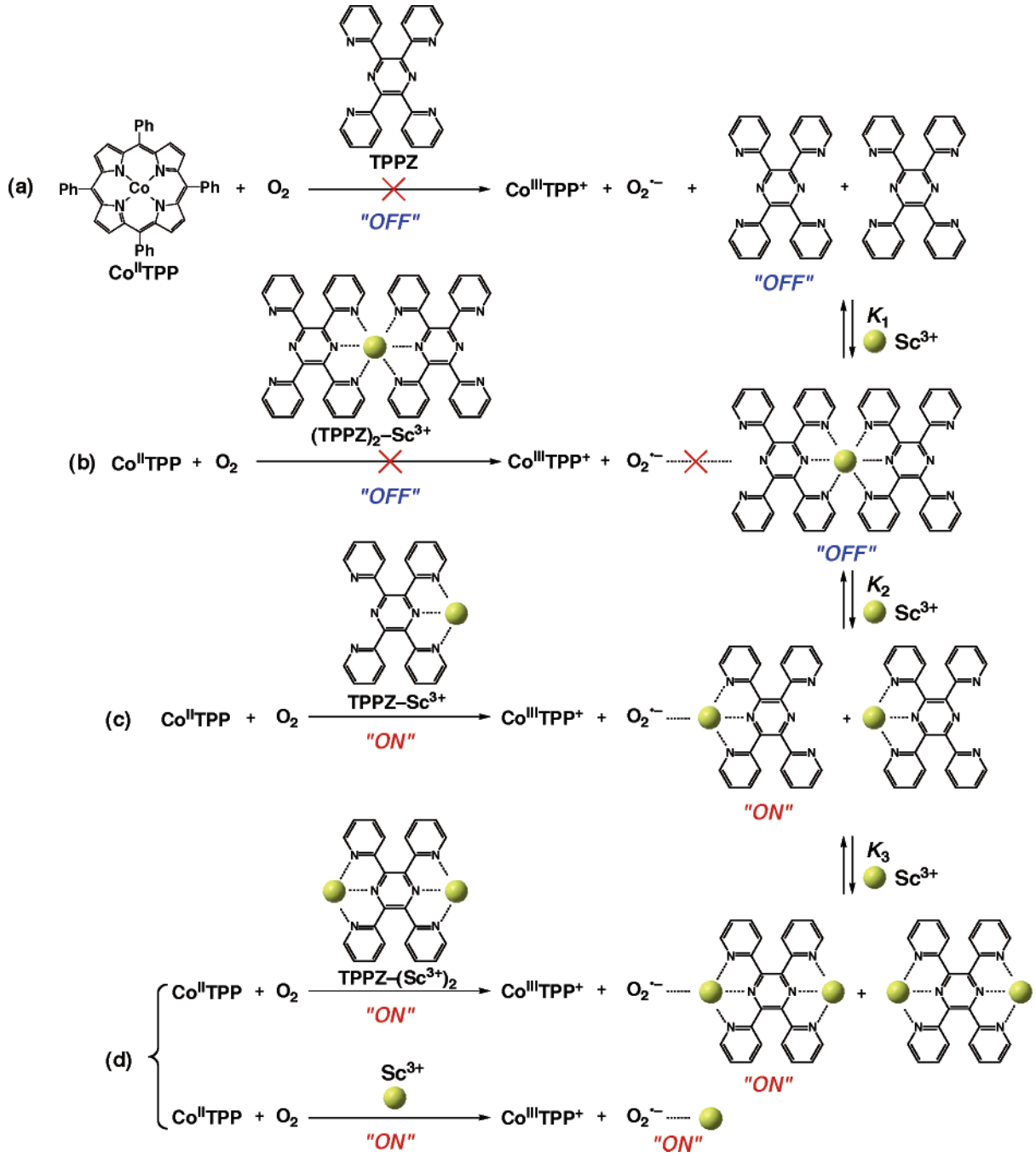

OFF−OFF−ON Switching in Metal Ion-Promoted Electron-Transfer Reduction of O_2. We have also examined the effects of stepwise complex formation of TPPZ with metal ions in metal ion-promoted electron transfer from CoTPP to O_2 (vide infra).[50] Since Sc^{3+} acting as strongest Lewis acid forms the 2:1 and 1:1 complexes stoichiometrically with TPPZ, the electron-transfer reduction of O_2 with CoTPP was examined in the presence of different ratios of Sc^{3+} to TPPZ.

No electron transfer from CoTPP (E_{ox} = 0.35 V vs SCE)[51] to O_2 (E_{red} = −0.86 V vs SCE)[52] has occurred in the presence of 0−0.5 equiv of Sc^{3+} ([Sc^{3+}]/[TPPZ]$_0$ < 0.5) in a deaerated MeCN solution of TPPZ (4.8×10^{-4} M) at 298 K. In the presence of more than 0.5 equiv of Sc^{3+} ([Sc^{3+}]/[TPPZ]$_0$ > 0.5), however, an efficient electron transfer from CoTPP to O_2 occurs to yield CoTPP$^+$. The rate of electron transfer was determined by monitoring a decrease in absorbance at 412 nm due to CoTPP and an increase in absorbance at 434 nm due to CoTPP$^+$. The rates obeyed pseudo-first-order kinetics in the presence of large excess of O_2, TPPZ, and Sc^{3+} relative to the concentration of CoTPP (see the first-order plot in Supporting Information S12). The pseudo-first-order rate constant (k_{obs}) increases proportionally with increasing O_2 concentration. The second-order rate constant of electron transfer (k_{et}) starts to increase at Sc^{3+} concentrations above the 1:2 ratio ([Sc^{3+}]/

(50) Metal ions acting as Lewis acids also accelerate the electron-transfer reduction of O_2, when metal ions bind with the product $O_2^{\bullet-}$; see ref 42.
(51) Fukuzumi, S.; Mochizuki, S.; Tanaka, T. *Inorg. Chem.* **1989**, *28*, 2459.
(52) Sawyer, D. T.; Calderwood, T. S.; Yamaguchi, K.; Angelis, C. T. *Inorg. Chem.* **1983**, *22*, 2577.

$[TPPZ]_0 > 0.5$) irrespective of the initial concentration of TPPZ [1.6×10^{-4} M (black closed circles), 3.2×10^{-4} M (red closed circles), and 4.8×10^{-4} M (blue closed circles)] as shown in Figure 9. Since Sc^{3+} complexes of TPPZ [$(TPPZ)_2-Sc^{3+}$ and $TPPZ-Sc^{3+}$] have no interaction with O_2, the promoting effects of Sc^{3+} on electron transfer at Sc^{3+} concentrations above the 1:2 ratio ($[Sc^{3+}]/[TPPZ]_0 > 0.5$) are ascribed to the complex formation of $TPPZ-Sc^{3+}$ with $O_2^{\bullet-}$.[53] The complex formation of $O_2^{\bullet-}$ and $TPPZ-Sc^{3+}$ should result in the positive shift of the one-electron reduction potential of O_2, leading to accelerate the electron-transfer reduction of O_2 (Scheme 3c).[50] In contrast to the case of $TPPZ-Sc^{3+}$, $(TPPZ)_2-Sc^{3+}$ (and TPPZ itself) cannot bind with $O_2^{\bullet-}$, since $(TPPZ)_2-Sc^{3+}$ has no binding site for $O_2^{\bullet-}$ (Scheme 3a,b). In such a case, no electron transfer from CoTPP to O_2 occurs at Sc^{3+} concentrations below the 1:2 ratio ($[Sc^{3+}]/[TPPZ]_0 < 0.5$). The 1:1 complex ($TPPZ-Sc^{3+}$) is further converted to the 1:2 complex $[TPPZ-(Sc^{3+})_2]$ in the presence of a large excess of Sc^{3+} (vide supra). In such a case, $TPPZ-(Sc^{3+})_2$ as well as excess free Sc^{3+} accelerate the electron-transfer reduction of O_2 by CoTPP (Scheme 3d), when the k_{et} values further increase with increasing Sc^{3+} concentrations above the 1:1 ratio ($[Sc^{3+}]/[TPPZ]_0 > 1$). The amount of excess free Sc^{3+} should vary depending on the initial concentration of TPPZ ($[TPPZ]_0$), because formation of the $TPPZ-(Sc^{3+})_2$ complex is not stoichiometric judging from the small formation constant [$K_3 = (2.2 \pm 0.1) \times 10^2$ M^{-1}; see Supporting Information S3]. This causes some deviations with regard to slopes above the 2:1 ratio ($[Sc^{3+}]/[TPPZ]_0 > 2$) (Figure 9).[54]

Summary and Conclusions

We have demonstrated OFF−OFF−ON switching of fluorescence and electron transfer depending on stepwise complex formation of TPPZ with metal ions (M^{n+}). Neither TPPZ itself nor the 2:1 complex $[(TPPZ)_2-M^{n+}]$ exhibits fluorescence (OFF). With increasing concentrations of metal ions, the $(TPPZ)_2-M^{n+}$ complex is converted to the 1:1 complex ($TPPZ-M^{n+}$) that exhibits strong fluorescence (ON). In the case of Sc^{3+}, which acts as the strongest Lewis acid among a series of examined metal ions, the $TPPZ-Sc^{3+}$ complex is further converted to the 1:2 complex $[TPPZ-(Sc^{3+})_2]$ at high concentration range of Sc^{3+}, which is also strongly fluorescent. Similarly, neither TPPZ nor the $(TPPZ)_2-Sc^{3+}$ complex has ability to promote electron transfer from CoTPP to O_2, which is thermodynamically infeasible (OFF). However, the electron transfer starts to occur (ON) at Sc^{3+} concentrations above the 1:2 ratio ($[Sc^{3+}]/[TPPZ]_0 > 0.5$), when the 2:1 complex $(TPPZ)_2-Sc^{3+}$ is converted to the 1:1 complex ($TPPZ-Sc^{3+}$) and the 1:2 complex is converted to $TPPZ-(Sc^{3+})_2$, which can bind strongly with $O_2^{\bullet-}$. Thus, TPPZ acts as unique ligands for metal ions, enabling "OFF−OFF−ON" switchability for metal ion fluorescence sensors and metal ion-promoted electron-transfer reactions.

Acknowledgment. This work was partially supported by Grants-in-Aid (No. 19205019) from the Ministry of Education, Culture, Sports, Science and Technology, Japan.

Supporting Information Available: UV−vis spectra of TPPZ in the presence of low and high concentrations of M^{n+} (S1 and S2, respectively), UV−vis spectra of TPPZ in the presence of Sc^{3+} (8.0×10^{-4} to 1.6×10^{-2} M) and the fluorescence spectrum of $TPPZ-(Sc^{3+})_2$ (S3), the optimized structures of $TPPZ-Mg^{2+}$ and $(TPPZ)_2-Mg^{2+}$ calculated by DFT at the B3LYP/6-31G** basis (S4), fluorescence titration of TPPZ by M^{n+} (S5), the derivation of eq 2 (S6), plots of $(1 - \alpha)^{-1}$ vs $[M^{n+}]/\alpha$ (S7), the derivation of eq 3 (S8) and eq 4 (S9), visible fluorescence of $TPPZ-Zn^{2+}$ in water (S10), time profiles of the fluorescence decay for $TPPZ-Sc^{3+}$, $TPPZ-Y^{3+}$, $TPPZ-Mg^{2+}$, and $TPPZ-Ca^{2+}$ (S11), and first-order plot for Sc^{3+}-promoted electron transfer from CoTPP to O_2 in the presence of TPPZ (S12). This material is available free of charge via the Internet at http://pubs.acs.org.

JA0748480

(53) We have previously reported ESR spectra of $O_2^{\bullet-}-Sc^{3+}$ complexes in fluid solution. See: Fukuzumi, S.; Patz, M.; Suenobu, T.; Kuwahara, Y.; Itoh, S. *J. Am. Chem. Soc.* **1999**, *121*, 1605.

(54) The slopes would be the same irrespective of the initial concentration of TPPZ at extremely high concentrations of Sc^{3+}, in which electron transfer is mainly promoted by excess free Sc^{3+}. However, the rate of electron transfer was too fast to be determined accurately at extremely high concentrations of Sc^{3+}.